Biological electric fields guide directional migration and promote epithelial–mesenchymal transition in lung cancer

Running title:EFs promote electrotaxis and EMT in lung cance

Conghua Lu[1, †],

Ying Zhang[1, †], Xiaolin Tang[1, †], Chen Hu[1], Xiaoli Jin[2], Bing Song[3, 4], Sanjun Zhao[2*], Yong He[1,*], Li Li[1,*]

Affiliations:

[1]Department of Respiratory Medicine, Daping Hospital, Third Military Medical University (Army Medical University), Chongqing, China

[2]School of Life Sciences, Yunnan Normal University, Kunming, China

[3]Institute of Biomedical and Health Engineering, Shenzhen Institutes of Advanced Technology, Chinese Academy of Sciences, Shenzhen, China.

[4]School of Dentistry, College of Biomedical and Life Sciences, Cardiff University, Cardiff CF14 4XY, UK.

† These authors contributed equally to this work.

*** Correspondence author:** Prof. Li Li, Department of Respiratory Medicine, Daping Hospital, Army Medical University, 400042, Chongqing, China. Phone: 86-23-68729190; Fax: 86-23-68729190; E-mail: dpyyhxlili@tmmu.edu.cn; or Prof. Yong He, Department of Respiratory Medicine, Daping Hospital, Army Medical University, 400042, Chongqing, China. E-mail: heyong@tmmu.edu.cn Prof. Sanjun Zhao, School of Life Sciences, Yunnan Normal University, 650500, Kunming, China, E-mail: sanjunzhao@hotmail.com

Keywords

Electric fields; Migration; Electrotaxis; Epithelial-mesenchymal transition; Lung cancer

Abstract

Endogenous direct-current electric fields (dcEFs), as one of the essential biophysical signals that naturally occur in the tumor microenvironment, were previously demonstrated to suppress the cytotoxicity of the third-generation tyrosine kinase inhibitor osimertinib in epidermal growth factor receptor (EGFR)-mutant lung cancer. In the current study, we further investigated the electrotactic response of EGFR-mutant lung cancer with different osimertinib sensitivity, including osimertinib-sensitive PC-9GR cells and osimertinib-resistant PC-9GROR cells. Firstly, in murine subcutaneous xenografts, robust endogenous electric currents were detected at the surface of tumors derived from osimertinib-resistant cells with a highly sensitive vibrating probe. Next, the electrotactic responses of two cell lines under EFs of different intensities were studied. Both PC-9GR and PC-9GROR cells exhibited directionally cathodal migration in a voltage-dependent manner, and osimertinib-resistant PC-9GROR cells displayed higher migration speeds. Epithelial-mesenchymal transition (EMT), which was previously reported to be closely related to tumor invasion and metastasis and could be suppressed by osimertinib, was enhanced under EF stimulation as reflected by increased vimentin and decreased E-cadherin in PC-9GR cells via western blotting and immunofluorescent staining regardless of osimertinib treatment. Additionally, pharmacological inhibition of PI3K/AKT signals reduced electrotaxis and EMT. Taken together, these results suggested that activation of AKT pathway may play an important role in electrotaxis and EMT of EGFR-mutant lung cancer.

Introduction

Lung cancer remains the leading cause of cancer-related deaths [1]. Epidermal growth factor receptor tyrosine kinase inhibitor (EGFR-TKI), such as the third-generation TKI osimertinib, has been recommended to be the standard therapy for advanced non-small cell lung cancer (NSCLC) patients with EGFR activating mutations [2]. Despite the excellent initial response, drug resistance in lung cancer inevitably occurs [3, 4]. As a complex entity that embeds cancer cells and multiple stromal cells, the tumor microenvironment has been reported to be associated with EGFR-TKI resistance [4, 5]. Endogenous electric fields (EFs) are one of the essential external biophysical signals of tumor microenvironment, which play a crucial part in the regulation of cell migration and can be mimicked by applied EFs of physiological strength [6-8]. Studies have reported that several types of lung cancer cells can migrate directionally under applied EFs, a phenomenon termed electrotaxis [9, 10]. Electrotaxis has been shown to participate in cancer metastasis[11]. For EGFR-mutant lung cancer, we previously reported that EFs inhibited pro-apoptotic effect of osimertinib through activating the AKT and forkhead box O3a (FOXO3a) with downstream decreased expression of Bim [12]. Epithelial-mesenchymal transition (EMT) is another major factor of cancer metastasis and a potential mechanism of acquired EGFR-TKI resistance [13, 14]. However, it is unclear how physiological EFs affect the directional migration and EMT of EGFR-mutant lung cancer with different osimertinib sensitivity.

In the current study, we first quantified and compared the intensity of electric currents in xenografts derived from two types of EGFR-mutant lung cancer cells, osimertinib-sensitive PC-9GR cells and osimertinib-resistant PC-9GROR cells. We further investigated the electrotactic responses and EMT of these two cell lines, and the role of AKT activation in the above processes.

Materials and methods

Xenografts establishment and vibrating probe measurement

The establishment of xenografts was performed as previously described [15]. The protocols were approved by the Ethics Committee of the Third Military Medical University. Briefly, 2 × 10^6 PC-9GR cells or PC-9GROR cells were injected subcutaneously into the back next to the left forelimb of 6-week-old female BALB/cA-nu mice (Laboratory Animal Center of Third Military Medical University, Chongqing, China). When tumors reached a size of ~100 mm^3 around day 14, the full-thickness dermal layer with the tumor was surgically removed from the tumor-bearing mice with surgical scissors after anesthetization and sacrifice of the mice. All samples were immersed in a 100mm-dish with mouse ringer solution (154 mM NaCl, 5 mM KCl, 2 mM $CaCl_2$, 1 mM $MgCl_2$, 11 mM D- Glucose, 5 mM HEPES buffer, pH 7.3, all from Sangon, Shanghai, China) for detection of electric currents. Endogenous electric current measurement using a non-invasive vibrating probe was performed as previously described [16]. The premade electrodes, obtained from World Precision Instruments (Sarasota, FL, USA), were plated with platinum (platinum chloride plating solution: 0.01% w/v lead acetate plus 1% H2PtCl6 6H2O in dH2O). A current of 200 nA was applied for 5 min, then increased to 500 nA for 2 min and 800 nA for 0.5 s until the probe tip reached the final tip size. The probe was calibrated with a reference electrode in mouse ringer solution before usage by applying a current of exactly 60 nA. The probe was calibrated again at the end of the procedure in the used solution to account for evaporation during the measurements. Using the Scanning Vibrating Electrode Technique (SVET system, Applicable Electronics, New Haven, CT, USA), the probe was vibrated at an amplitude that approximates twice the tip's diameter, and the motion of the probe was in a straight line not exceeding 20 degrees away from

the true axis perpendicular to the measure site. All procedures followed the SVET system manual. The full-thickness dermal layer with the tumor was fixed at the bottom of the measuring chamber with high vacuum grease (Down Corning, USA). The electric currents were measured independently at the tumor site and normal skin adjacent to the tumor as a control.

Cell lines

Gefitinib-resistant PC-9GR cells were generously provided by Prof. J. Xu and Dr. M. Liu (Guangzhou Medical University, China). Lung adenocarcinoma H1975 cells were purchased from American Type Culture Collection (ATCC). To establish osimertinib-resistant PC-9GROR cell lines, the parental cells were treated with osimertinib at the concentration of IC50 for 2 weeks, with higher drug levels for another 3 weeks. The latter dosage was sufficient to kill all parental cells. When resistant clones were visible, the cells were diluted to a single cell per well, and continuous culture was performed in the presence of osimertinib at IC50. All cells were cultured in RPMI-1640 (Hyclone) with Earle's salts, supplemented with 10% FBS (Gibco), 2 mmol/L L-glutamine (Gibco), 100U/ml penicillin (HyClone), and 100μg/mL streptomycin (Hyclone) at 37°C, with 5% CO2 and 90% humidity.

Reagents

Osimertinib (TAGRISSO) was obtained from Astra Zeneca. LY294002 was purchased from Selleck. Anti-total-AKT (#4685), phospho-(Ser473)-AKT (#4060), E-cadherin (14472), vimentin (#5741), GAPDH (#2118S) antibodies were from Cell Signaling Technology.

Electrical field stimulation and drug treatment

Methods of applying EFs have been described previously [17]. Briefly, cells were seeded into a 6-well cell culture plate (tissue culture treated, Corning incorporation, NY, USA) and allowed to adhere overnight in a 5% CO_2 incubator. A coverglass was subsequently applied as a roof and sealed with high vacuum silicone grease (Dow Corning Corp., Midland, MI, USA) so that the final dimensions of the chamber were 24 mm × 10 mm × 0.2 mm. CO_2-independent culture medium (Gibco) plus 10% FBS was used to maintain stable pH. Direct current was applied through agar-salt bridges connecting silver/silver chloride electrodes in Steinberg's solution to pooled medium on each side of the electrotaxis chamber. Cells were exposed to 0-200 mV/mm steady EFs for the indicated periods. Time-lapse images were acquired using ImageXpress Micro (Molecular Devices) high-throughput imager.

Cells were treated with LY294002 (20μM) or osimertinib (0.5μM) for 24 hours. After that,medium was changed and CO_2-independent culture medium was added. Then those cells were exposed to an EF of 100 mV/mm for 1 hour in the presence of the indicated inhibitors.

Quantitative analysis of cell migration

Cell migration was quantified using ImageJ software (NIH, Bethesda, MA, USA) with MTrackJ and Chemotaxis tool plugins as previously described [18]. Directedness ($\cos\theta$) represents how directionally the cells migrated, where θ is the angle between the field vector and the cell migration direction. The average directedness value reflects the directionality of a group of cells. The directedness values close to 0 indicated that cells had migrated randomly, and those close to 1 or −1 indicated the movement of cells towards the anode or the cathode, respectively. Cell migration speed was quantified as trajectory speed (Tt/t, in μm/h), as calculated by the total length of the migration trajectory of a cell (Tt) divided by the given period of time.

Western blot assay

Cells harvested by scraping were washed twice with PBS and lysed for 30 min at 4°C in RIPA buffer (Sigma-Aldrich,France). After centrifugation at 12000g for 15 min at 4°C, the protein concentrations were determined by the BCA assay. Equal amounts of protein were applied to gel electrophoresis for 2 h at 110 V, followed by transferring to PVDF membranes (90 min,200 mA) (Millipore,German). Membranes were blocked with 5% bovine serum albumin (BSA) for 1 h at room temperature and incubated overnight at 4°C with primary antibodies. Subsequently, the membranes were washed and incubated with 0.02 μg/ml horseradish peroxidase (HRP)-conjugated goat anti-rabbit or anti-mouse IgG (Sino Biological, China) for 1 h, and visualized with ChemiDoc Touch System (Bio-Rad,USA).

Immunofluorescent staining

For immunofluorescence, cells were washed with PBS and fixed in 4% paraformaldehyde at room temperature for 30 min. Non-specific binding was blocked using 10% normal goat serum (Sigma). Cells were incubated with the following primary antibodies after being diluted in PBS with 1% bovine serum albumin at 4°C overnight: rabbit monoclonal vimentin and mouse monoclonal E-cadherin (Cell Signaling Technology). Then, cells were washed twice with PBS and incubated with secondary antibodies at 37°C for 30 min as follows: FITC-conjugated goat-anti-rabbit IgG (Abcam, Cambridge, UK). The slides were mounted in mounting medium with 4',6-diamidino-2-phenylindole (DAPI; Solarbio, Beijing, China) and viewed with ImageXpress Micro (Molecular Devices) high-throughput imager.

Statistical analysis

All data are presented as mean ± standard error of mean (SEM). Statistical analysis was performed by an unpaired, two-tailed Student's t-test and statistical significance was assumed at an alpha value of $p < 0.05$.

Results

Osimertinib-resistant tumor xenografts enhanced endogenous electric currents

To map the electric currents in lung tumors with different sensitivity to osimertinib, we established a cell line derived tumor xenograft (CDX) model with PC-9GR and PC-9GROR cells subcutaneously injecting into mice and monitored for two weeks. We then measured electric currents at the surface of the CDX tumors using a non-invasive vibrating probe system (Figure 1A). Stronger inward electrical currents were detected at the surface of xenografts when compared with control skin. In contrast, a remarkably stronger current intensity was detected in tumor derived from osimertinib-resistant cells (Figure 1B), indicating the CDX lung tumors indeed generated an electric field at the surface and appeared to have a potential link with osimertinib resistance.

EFs induced directional migration of lung cancer cells towards cathode

Electrotaxis of tumor cells was cell-type dependent and associated with their metastatic capability [19]. Herein, we investigated electrotactic response (directedness and speed) of EGFR-mutant lung cancer cells with different drug sensitivity. PC-9GR cells and PC-9GROR cells were exposed with different EF stimulation ranging between 50-200 mV/mm. Both cell types were either left untreated as control or exposed to EFs for four hours, respectively. Compared with control group which migrated randomly with a low trajectory speed, EF-treated cells showed a cathodal migration at 50mV/mm and a progressive directedness and speed with the increase in EF strengths as reflected in single cell tracking analysis (Figure 2A and B, Supplementary FigureS1 and

Supplementary Movie 1 and 2). Both PC-9GR and PC-9GROR cells had a significantly higher migration speed under EF explosure and the migration speeds were also increased by stimulation with higher EF. Interestingly, PC-9GROR cells displayed higher migratory speed compared with PC-9GR cells, especially at higher EF (Figure 2C). When exposed to the same strength of EF stimulation, there was no significant difference in directedness between PC-9GR and PC-9GROR cells below 100 mV/mm. In contrast, 100 mV/mm EF triggered a higher directedness approaching -1 in PC-9GROR cells compared to PC-9GR cells (PC-9GROR vs. PC-9GR: -0.8875 ± 0.0217 vs. -0.63 ± 0.0505; P = 0.0013). When the strength was up to 200 mV/mm, both PC-9GR and PC-9GROR cells exhibited the highest directedness while there was no significant difference between the two cell types (PC-9GROR vs. PC-9GR: -0.9256 ± 0.01037 vs. -0.93 ± 0.0093; P = 0.5680. Figure 2D). Taken together, these data suggested that EFs could guide robust directional migration of PC-9GR and PC-9GROR cells in an EF strength-dependent manner.

EF stimulation promoted EMT in lung cancer cells

Considering that cell migration could be enhanced by EMT, which was a dynamic and reversible cellular program and closely related to carcinogenesis and tumor metastasis by enhancing mobility, invasion and resistance to apoptotic stimuli of cancer cells [20], as well as EGFR-TKI resistance via activation of various intracellular signaling pathway [13, 21], we next investigated the impact of osimertinib and EFs on EMT. As shown in Figure 3A and Supplementary Figure S4A, western blotting revealed that in osimertinib-sensitive PC-9GR cells or H1975 cells, EF stimulation increased vimentin expression, which was one of the mesenchymal phenotypical markers. In contrast, the E-cadherin, an epithelial phenotypical marker, was decreased after EF stimulation. Although osimertinib increased E-cadherin and decreased

vimentin expression in osimertinib-sensitive PC-9GR cells, EMT was re-enhanced after applying an EF (Figure 3B and Supplementary Figure S4B). These results were confirmed by immunofluorescent staining (Figure 3C and Supplementary Figure S2). Put together, these findings indicated that EF stimulation could reverse osimertinib-inhibited EMT in osimertinib-sensitive lung cancer cells.

AKT phosphorylation is required in EFs-induced electrotaxis and EMT of lung cancer cells

Various studies have proved that AKT is one of the key signaling pathways involved in cell proliferation, apoptosis and migration during cancer development [22]. We previously reported that EFs attenuated pro-apoptotic effect of osimertinib by enhancing the phosphorylation level of AKT/FOXO3a[12]. In this study, we then investigated whether AKT activation was involved in electrotaxis and EFs-mediated EMT in EGFR-mutant lung cancer cells.

As reported in our previous study, proteomics analysis exhibited a higher activation level of AKT pathway in PC-9GROR cells compared with PC-9GR cells[15]. We therefore assessed EF-induced activation of AKT pathway. Western blotting results demonstrated that EF enhanced the phosphorylation of AKT in lung cancer cells without altering the total expression of AKT (Figure 4A and and Supplementary Figure S4C). Next, we investigated whether EF-induced AKT phosphorylation was involved in the regulation of cell migration using LY294002, a PI3K/AKT inhibitor. PC-9GR and PC-9GROR cells were pretreated with LY294002 (20μM) for 24 hours and then exposed to EF of 100 mV/mm for 1 hour(Figure 4B). Quantitative analysis of cell migration in Figure 4C and 4D showed that LY294002 significantly decreased the migration speed of PC-9GR and PC-9GROR cells in the presence of EF stimulation. As for the

migration directedness, in view of the extremely small movements of PC-9GR and PC-9GROR cells when treated with LY294002, even shorter than their own diameters, the direction is very difficult to discern. Thus the role of EFs on the migration directedness in the presence of LY294002 remained uncertain. The dynamic movements of cells were presented in time-lapse photographs (Supplementary Figure S3). Similarly, as a key step for cell migration, EF-promoted EMT in PC-9GR and PC-9GROR cells also could be reversed by LY294002 as shown in both western blotting results and immunofluorescent staining (Figure 5 and Supplementary Figure S4D). Collectively, these results above suggested that AKT activation played an essential role in electrotaxis and EF-promoted EMT in EGFR-mutant lung cancer cells (Figure 6).

Discussion

In the present study, we demonstrated that endogenous EFs existed at the surface of EGFR-mutant lung tumor xenografts, and stronger current intensity was found in tumors derived from osimertinib-resistant cells. Both osimertinib-resistant and osimertinib-sensitive lung cancer cells showed electrotaxis in a strength-dependent manner, while higher migration speeds were found in osimertinib-resistant cells under an EF of the same intensity. Furthermore, EFs induced EMT and AKT activation, and AKT activation was required for electrotaxis and EF-enhanced EMT of lung cancer cells. Taken together, these data suggest that AKT activation is needed for EFs-induced directional migration and EMT in EGFR-mutant lung cancer cells.

As one of the biophysical signals, endogenous dcEF has been detected in epithelial wounds and many tumor tissues [8, 23]. Nasal potential difference measurement is easily performed in humans with good tolerance, which has been used as a diagnostic technique in cystic fibrosis for over 25 years [24]. Moreover, the potential difference in the human lower airway has also been

successfully measured using microelectrodes via the bronchoscope [25], which correlates closely with the nasal potential difference. However, these have not been applied to lung cancer. In addition, the measurement of alveolar potential difference requires alveolar micropuncture with microelectrode insertion, which would be invasive and difficult to achieve. In this study, we detected the electric currents at the surface of subcutaneous lung tumor xenografts by a non-invasive vibrating probe system, which could be used on patients without risk of ionising radiation. In the future, combining advanced electromagnetic navigation bronchoscopy with more non-invasive probe systems is expected to promote the development of precise measurement of the bioelectric signaling even at the deep site of lung lesions throughout tumor initiation, promotion and metastasis. However, the lack of the intratumor electric potential measurements makes the mechanisms of the generation of the endogenous EFs uncertain. The intratumor electric potential reflects the electrical property of the tumor, and the potential difference between the outside surface and inside of the tumor results in the endogenous EFs that flowing inside or outside of the tumors, which may affect cell migration and ultimately contribute to cancer metastasis[6]. Besides, we cannot rule out the possibility that other factors such as inflammation and neovascularization of the overlying epidermis lead to the measurement results by the SVET rather than the tumor's independent properties.

Electrotaxis is of significance in cancer invasion and metastasis. Membrane potential is the basic level of bioelectricity generated in single cell, which has been suggested to regulate cancer cell proliferation, migration, and differentiation[26]. Resting membrane potential is more depolarized in cancer cells compared to normal cells, and the potential difference between the non-proliferative region and the proliferative region subsequently generates an endogenous electric field in the tumor microenvironment [27, 28]. Invasion of

lung cancer cells into the bronchi results in deformation of the epithelium, which then leads to short-circuit trans-epithelial potential and generates endogenous EFs. Next, EFs further promote the invasion of cancer cells in a feedback cycle, which potentiates lung cancer metastasis to bronchial lumen or even other tissues. Previously, one study demonstrated that the highly invasive lung adenocarcinoma cells displayed a higher migration directionality and speed than the low invasive ones [29], which was similar to our finding that a higher migration speed is shown in PC-9GROR cells compared with PC-9GR cells under the same EF stimulation. Other studies also suggested that electrotaxis was considered to be correlated with metastatic capability [7, 19]. In addition, under the EF stimulation below 100 mV/mm, which was considered as the physiologically important endogenous EF strength[30], the directionality between the PC-9GR and PC-9GROR cells showed no much difference. Another breast cancer models showed similar results that the directedness of most sublines was comparable with the parental cells in an EF below 100 mV/mm. These phenomena may indicate that physiologically endogenous EF is more likely to influence the rate of metastasis rather than metastatic sites. However, there were different electrotaxis thresholds among parental cells and metastatic sublines. Parental mammary carcinoma cell line and lung metastatic sublines could respond to EF as low as 50 mV/mm, while other metastatic sublines from lymph node, spleen, and heart showed weaker responses, which indicated an abnormal sensing of weak EF or a disorder of electrophysiological state may effect local invasion and metastatic dissemination[6]. As shown in our results, a remarkably stronger current intensity was generated in tumor derived from osimertinib-resistant cells and PC-9GROR cells had a higher migratory speed, which may indicate a higher risk of metastasis in a drug-resistant tumor microenvironment since EFs could guide robust directional migration of lung cancer cells in an EF strength-dependent manner. These data

revealed a crosstalk between metastasis and drug resistance, pointing out a direction for inhibiting the tumor metastasis induced by drug resistance through regulating EFs.

In the current study, we found that the AKT pathway was required for electrotaxis and EF-enhanced EMT in EGFR-mutant lung cancer cells. Previously, EGFR downstream intracellular signaling cascades including cyclic AMP (cAMP), the tumour suppressor phosphatase and tensin homolog (PTEN), ERK MAP kinase (ERK1/2) and calcium signaling have also been reported to play a role in electrotaxis[10, 31-33]. These reports spark interest in further exploring other parallel signaling pathways to coordinate electrotaxis and EMT of lung cancer cells. Besides, EFs were previously identified to result in asymmetric distribution of receptor tyrosine kinases (RTKs) located on the cell membrane[19], which could bind to various growth factors. Meanwhile, phosphorylation of RTKs is known to activate the downstream signaling cascade of PI3K/AKT and MAPK pathways[34] , which suggests a possible inter-relationship between electrotaxis and chemotaxis via RTKs. Future research is expected to comprehensively clarify multi-intracellular signaling dynamics involved in electrotaxis.

Conclusions

Collectively, our study adds to the current knowledge about EGFR-mutant lung cancer invasion and metastasis from a biophysical perspective. A thorough understanding of the underlying bioelectric mechanisms and precise regulation of endogenous EFs may ultimately help to develop a brand-new therapeutic strategy to enhance EGFR-TKI efficacy and improve the prognosis of NSCLC patients with EGFR mutations.

Conflict of interest

The authors declare that they have no conflict of interest.

Funding

This work was supported by National Natural Science Foundation of China (82272908, 81672287), Natural Science Foundation of Chongqing (CSTB2022NSCQ-MSX1110), Guangdong Association of Clinical Trials (GACT), Daping Hospital of Army Medical University (2019CXJSB004, 2019CXLCB011). The funders had no role in study design, data collection and analysis, decision to publish, or preparation of the manuscript.

References

1. Siegel RL, Miller KD, Fuchs HE, et al: **Cancer statistics, 2022.** *CA Cancer J Clin* 2022, **72**, 7-33, doi:10.3322/caac.21708.
2. Soria JC, Ohe Y, Vansteenkiste J, et al: **Osimertinib in Untreated EGFR-Mutated Advanced Non-Small-Cell Lung Cancer.** *N Engl J Med* 2018, **378**, 113-125, doi:10.1056/NEJMoa1713137.
3. Meador CB, Hata AN: **Acquired resistance to targeted therapies in NSCLC: Updates and evolving insights.** *Pharmacol Ther* 2020, **210**, 107522, doi:10.1016/j.pharmthera.2020.107522.
4. Wu J, Lin Z: **Non-Small Cell Lung Cancer Targeted Therapy: Drugs and Mechanisms of Drug Resistance.** *Int J Mol Sci* 2022, **23**, doi:10.3390/ijms232315056.
5. Jia Y, Li X, Jiang T, et al: **EGFR-targeted therapy alters the tumor microenvironment in EGFR-driven lung tumors: Implications for combination therapies.** *Int J Cancer* 2019, **145**, 1432-1444, doi:10.1002/ijc.32191.
6. Zhu K, Hum NR, Reid B, et al: **Electric Fields at Breast Cancer and Cancer Cell Collective Galvanotaxis.** *Sci Rep* 2020, **10**, 8712, doi:10.1038/s41598-020-65566-0.
7. Mycielska ME, Djamgoz MB: **Cellular mechanisms of direct-current electric field effects: galvanotaxis and metastatic disease.** *J Cell Sci* 2004, **117**, 1631-1639, doi:10.1242/jcs.01125.
8. Payne SL, Levin M, Oudin MJ: **Bioelectric Control of Metastasis in Solid Tumors.** *Bioelectricity* 2019, **1**, 114-130, doi:10.1089/bioe.2019.0013.
9. Yan X, Han J, Zhang Z, et al: **Lung cancer A549 cells migrate directionally in DC electric fields with polarized and activated EGFRs.** *Bioelectromagnetics* 2009, **30**, 29-35, doi:10.1002/bem.20436.
10. Li Y, Yu WK, Chen L, et al: **Electrotaxis of tumor-initiating cells of H1975**

lung adenocarcinoma cells is associated with both activation of stretch-activated cation channels (SACCs) and internal calcium release. *Bioelectrochemistry* 2018, **124**, 80-92, doi:10.1016/j.bioelechem.2018.03.013.

11. Levin M: **Bioelectric signaling: Reprogrammable circuits underlying embryogenesis, regeneration, and cancer.** *Cell* 2021, **184**, 1971-1989, doi:10.1016/j.cell.2021.02.034.
12. Li L, Hu C, Lu C, et al: **Applied electric fields suppress osimertinib-induced cytotoxicity via inhibiting FOXO3a nuclear translocation through AKT activation.** *Carcinogenesis* 2020, **41**, 600-610, doi:10.1093/carcin/bgz150.
13. Zhu X, Chen L, Liu L, et al: **EMT-Mediated Acquired EGFR-TKI Resistance in NSCLC: Mechanisms and Strategies.** *Front Oncol* 2019, **9**, 1044, doi:10.3389/fonc.2019.01044.
14. Dzul Keflee R, Leong KH, Ogawa S, et al: **Overview of the multifaceted resistances toward EGFR-TKIs and new chemotherapeutic strategies in non-small cell lung cancer.** *Biochem Pharmacol* 2022, **205**, 115262, doi:10.1016/j.bcp.2022.115262.
15. Li L, Li Z, Lu C, et al: **Ibrutinib reverses IL-6-induced osimertinib resistance through inhibition of Laminin alpha5/FAK signaling.** *Commun Biol* 2022, **5**, 155, doi:10.1038/s42003-022-03111-7.
16. Reid B, Zhao M: **Measurement of bioelectric current with a vibrating probe.** *J Vis Exp* 2011, doi:10.3791/2358.
17. Lin F, Rajnicek A, Zhao M: **Methodology of Research and Applications of Electric Fields.** *Bioelectricity* 2020, **2**, 320, doi:10.1089/bioe.2020.0050.
18. Zhao Z, Zhu K, Li Y, et al: **Optimization of Electrical Stimulation for Safe and Effective Guidance of Human Cells.** *Bioelectricity* 2020, **2**, 372-381, doi:10.1089/bioe.2020.0019.
19. McCaig CD, Song B, Rajnicek AM: **Electrical dimensions in cell science.** *J Cell Sci* 2009, **122**, 4267-4276, doi:10.1242/jcs.023564.
20. Zhao R, Wu Z, Zhou Q: **[Epithelial-mesenchymal transition and tumor metastasis].** *Zhongguo Fei Ai Za Zhi* 2011, **14**, 620-624, doi:10.3779/j.issn.1009-3419.2011.07.11.
21. Yochum ZA, Cades J, Wang H, et al: **Targeting the EMT transcription factor TWIST1 overcomes resistance to EGFR inhibitors in EGFR-mutant non-small-cell lung cancer.** *Oncogene* 2019, **38**, 656-670, doi:10.1038/s41388-018-0482-y.
22. Larue L, Bellacosa A: **Epithelial-mesenchymal transition in development and cancer: role of phosphatidylinositol 3' kinase/AKT pathways.** *Oncogene* 2005, **24**, 7443-7454, doi:10.1038/sj.onc.1209091.
23. Levin M: **The wisdom of the body: future techniques and approaches to morphogenetic fields in regenerative medicine, developmental**

biology and cancer. *Regen Med* 2011, **6**, 667-673, doi:10.2217/rme.11.69.
24. Mac Sweeney R, Fischer H, McAuley DF: **Nasal potential difference to detect Na+ channel dysfunction in acute lung injury.** *Am J Physiol Lung Cell Mol Physiol* 2011, **300**, L305-318, doi:10.1152/ajplung.00223.2010.
25. Davies JC, Davies M, McShane D, et al: **Potential difference measurements in the lower airway of children with and without cystic fibrosis.** *Am J Respir Crit Care Med* 2005, **171**, 1015-1019, doi:10.1164/rccm.200408-1116OC.
26. Yang M, Brackenbury WJ: **Membrane potential and cancer progression.** *Front Physiol* 2013, **4**, 185, doi:10.3389/fphys.2013.00185.
27. Berzingi S, Newman M, Yu HG: **Altering bioelectricity on inhibition of human breast cancer cells.** *Cancer Cell Int* 2016, **16**, 72, doi:10.1186/s12935-016-0348-8.
28. Djamgoz MB, Coombes RC, Schwab A: **Ion transport and cancer: from initiation to metastasis.** *Philos Trans R Soc Lond B Biol Sci* 2014, **369**, 20130092, doi:10.1098/rstb.2013.0092.
29. Tsai HF, Huang CW, Chang HF, et al: **Evaluation of EGFR and RTK signaling in the electrotaxis of lung adenocarcinoma cells under direct-current electric field stimulation.** *PLoS One* 2013, **8**, e73418, doi:10.1371/journal.pone.0073418.
30. Hart FX: **The mechanical transduction of physiological strength electric fields.** *Bioelectromagnetics* 2008, **29**, 447-455, doi:10.1002/bem.20411.
31. Matsubayashi Y, Ebisuya M, Honjoh S, et al: **ERK activation propagates in epithelial cell sheets and regulates their migration during wound healing.** *Curr Biol* 2004, **14**, 731-735, doi:10.1016/j.cub.2004.03.060.
32. Pullar CE, Isseroff RR: **Cyclic AMP mediates keratinocyte directional migration in an electric field.** *J Cell Sci* 2005, **118**, 2023-2034, doi:10.1242/jcs.02330.
33. Zhao M, Song B, Pu J, et al: **Electrical signals control wound healing through phosphatidylinositol-3-OH kinase-gamma and PTEN.** *Nature* 2006, **442**, 457-460, doi:10.1038/nature04925.
34. Pu J, McCaig CD, Cao L, et al: **EGF receptor signalling is essential for electric-field-directed migration of breast cancer cells.** *J Cell Sci* 2007, **120**, 3395-3403, doi:10.1242/jcs.002774.

Figure legends

Figure 1. Electrical currents at tumors ex vivo. A) Murine EGFR-mutant xenografts derived from two types of cells and the following measurement of electrical currents using vibrating probe. B) Electrical currents detected at the surface of skin and tumors from PC-9GR and PC-9GROR xenograft groups. **P < 0.01 compared with PC-9GR cells. ##P< 0.01 as compared with the skin. PC-9GR and PC-9GROR cells were injected s.c. into nude mice (2×10^6 cells per mouse, n = 3) for 2 weeks. The volume of tumors was measured every 2 days. Scale bar = 3 mm. Three replicate measurements were made at each turmor, data are shown as mean ± S.E.M.

Figure1

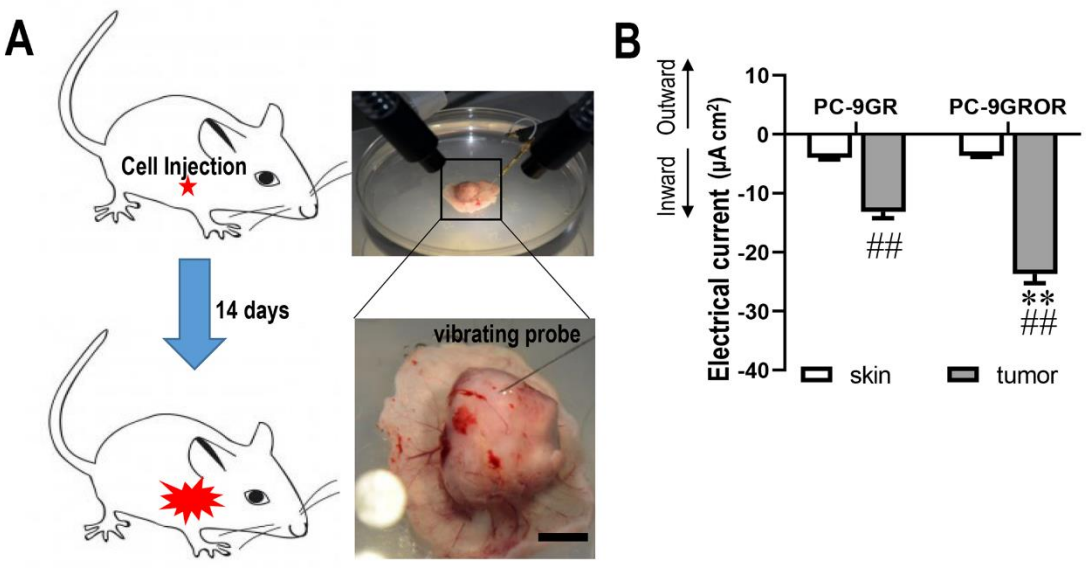

Figure 2. Electric fields guided cell directional migration. A) Time lapse photographs of PC-9GR and PC-9GROR cells in the presence of EFs for 4 hrs. Red lines and yellow arrows represent migration paths and direction respectively. Scale bars = 50 μm. B) The migration trajectory of PC-9GR and PC-9GR OR cells under a series of EF. EF direction was from right to left and initial cell positions were set at 0. C) Migration speeds of PC-9GR and PC-

9GROR cells were indicated by velocity (bar chart). *P < 0.05 and **P < 0.01 vs. No EF group, ##P< 0.01 as compared with that of 50 mV/mm, showing significant difference. D) Directedness (cosθ) of PC-9GR and PC-9GROR cells in the absence or presence of EF stimulation. θ is the angle between the field vector and the cell migration direction. Data are derived from at least 100 cells from three independent experiments and shown as mean ± S.E.M. *P < 0.05 and **P < 0.01 vs. No EF group, ##P< 0.01 as compared with that of 50 mV/mm.

Figure2

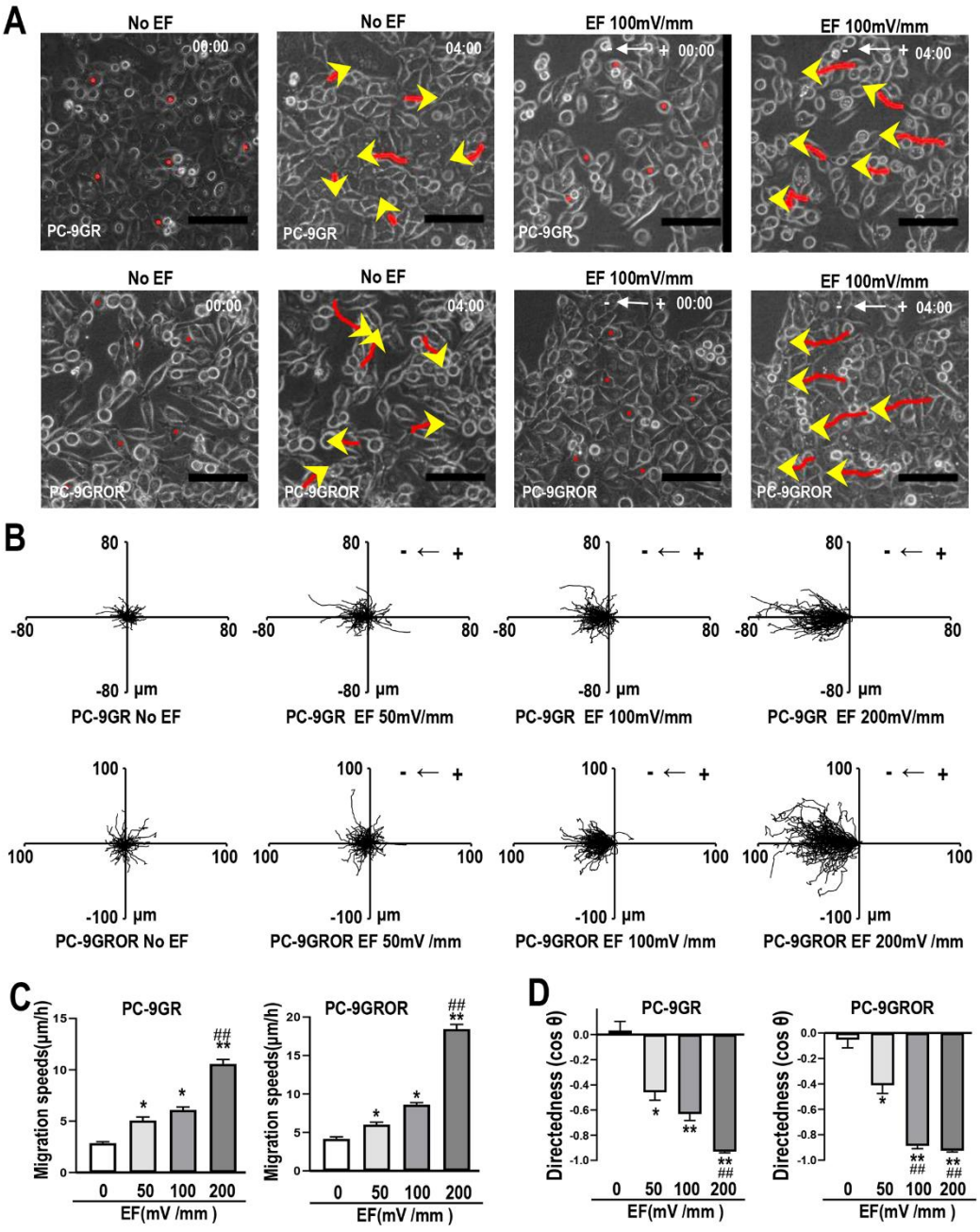

523

524 **Figure 3.** EF promoted osimertinib-inhibited EMT in osimertinib-sensitive lung
525 cancer cells. A) Expressions of epithelial phenotypical protein E-cadherin and
526 mesenchymal phenotypical proteins vimentin were detected by western blotting
527 in PC-9GR cells and H1975 cells with GAPDH as a loading control. Both of
528 which showed a decreased level of E-cadherin and an increased level of
529 vimentin under the stimulation of EF. B) Followingly, osimertinib treatment

suppressed the expression of vimentin but increased the level of E-cadherin in PC-9GR while this got reversed after applying EF. Similar results were obtained from three independent experiments. C) PC-9GR cells were stained for E-cadherin, vimentin and DAPI and viewed with ImageXpress Micro. The green signal represents staining for E-cadherin while the red signal signifies vimentin. Scale bars = 50 μm.

Figure3

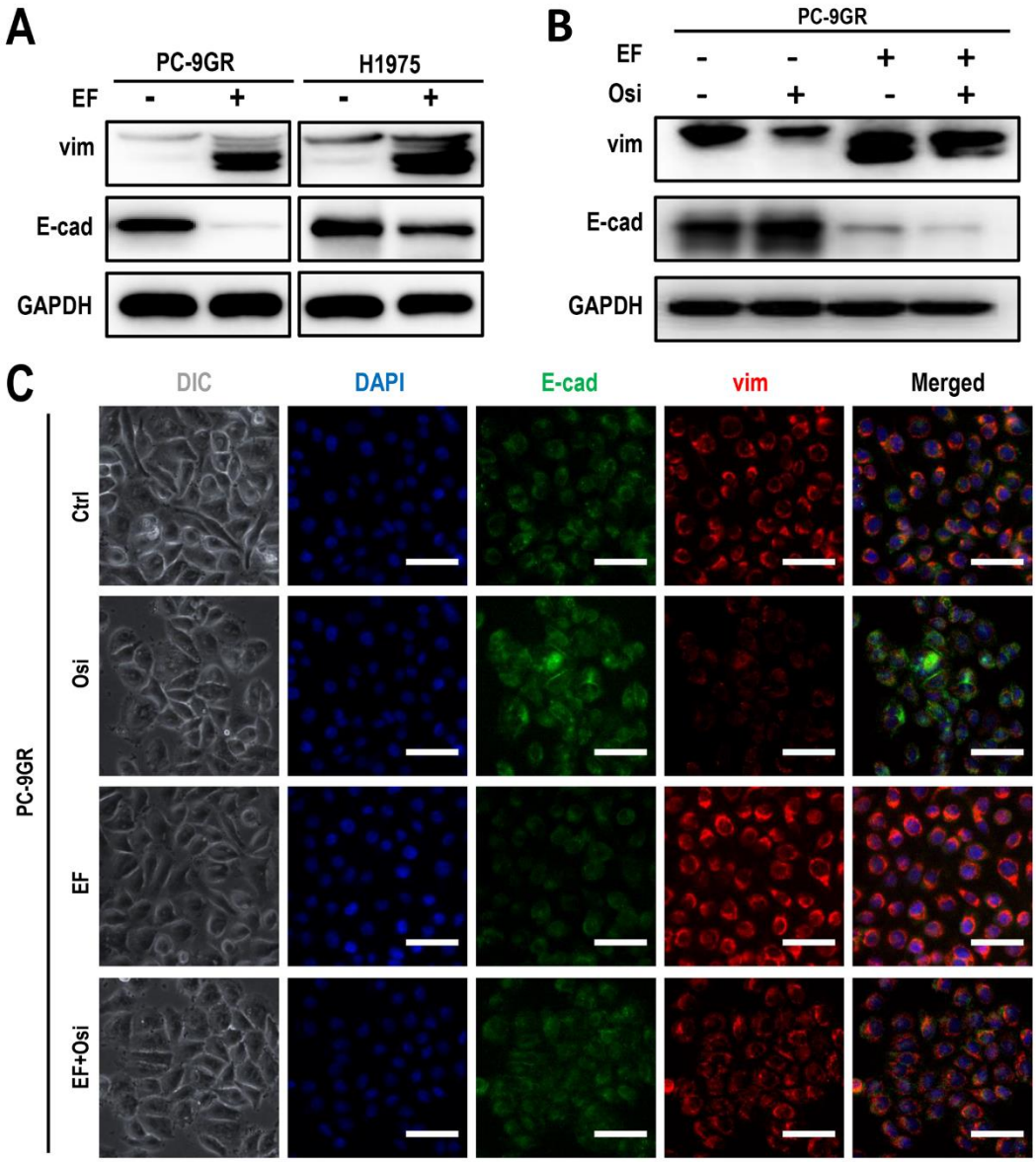

Figure 4. AKT pathway was required for EF-guided directional migration. A) Phosphorylation level of AKT when given EF or/with LY294002 was shown by

western blotting bands with GAPDH as a loading control. Similar results were obtained from three independent experiments. B) The migration trajectory of PC-9GR and PC-9GROR cells. C) and D) Directedness (cosθ) and migration speeds of PC-9GR and PC-9GROR cells were indicated by velocity (bar chart). **P < 0.01 vs. No EF group, ##P< 0.01 vs. EF group, showing a significant difference. Data are from at least 100 cells from three independent experiments and shown as mean ± S.E.M.

Figure4

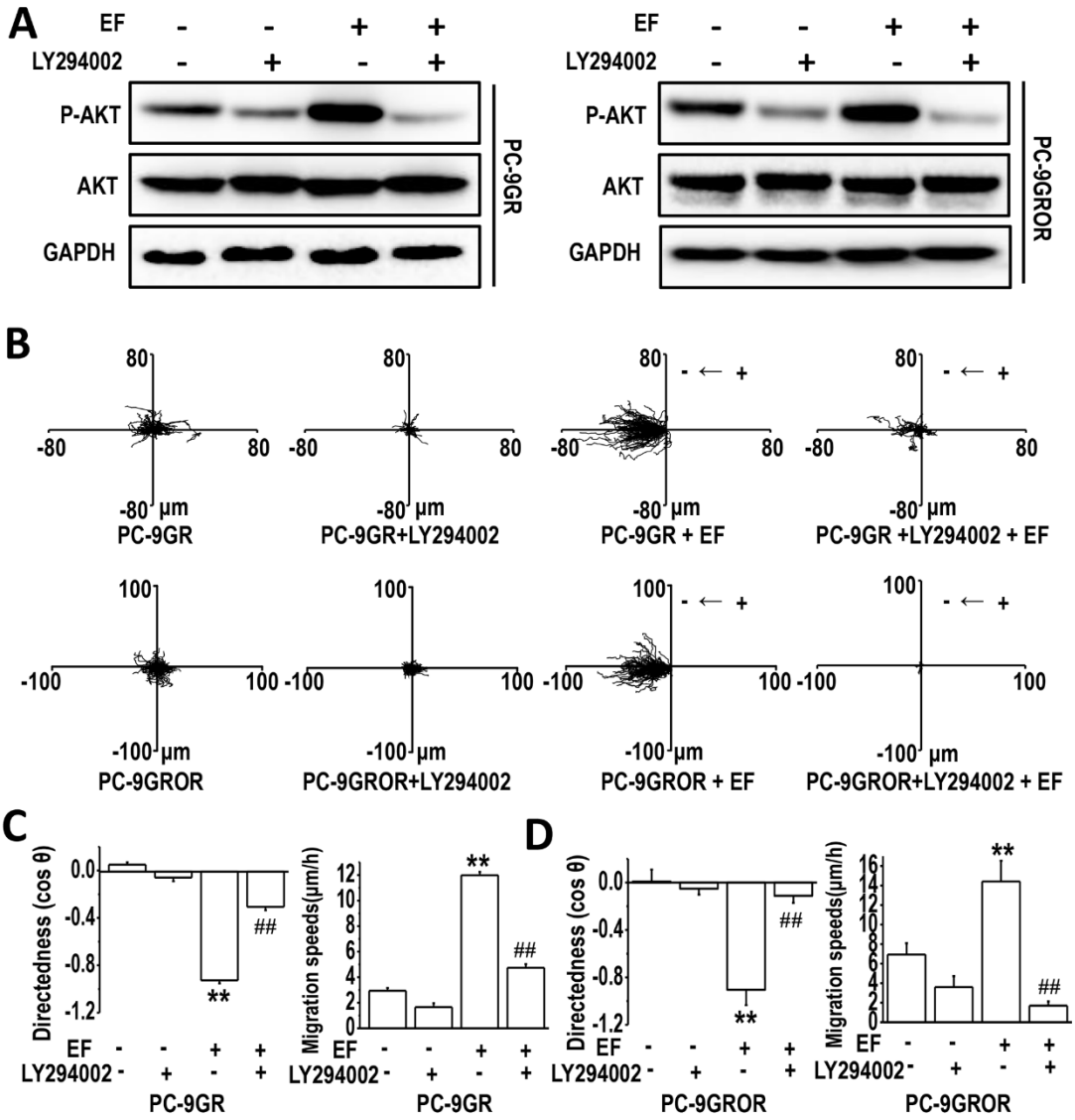

Figure 5. AKT activation was required for EF-stimulated EMT. A) Expressions

of epithelial phenotypical protein E-cadherin and mesenchymal phenotypical protein vimentin were detected by western blotting in PC-9GR and PC-9GROR cells, both of which were given EF or/with LY294002. GAPDH was used as a loading control. Similar results were obtained from three independent experiments. B) Immunofluorescence characterization of EMT phenotypical proteins under the treatment of EF or/with LY294002, showing the condition of EMT. The nucleus was counterstained with DAPI. (Red, vimentin; Green, E-cadherin; Blue, DAPI). Scale bars = 50 μm.

Figure5

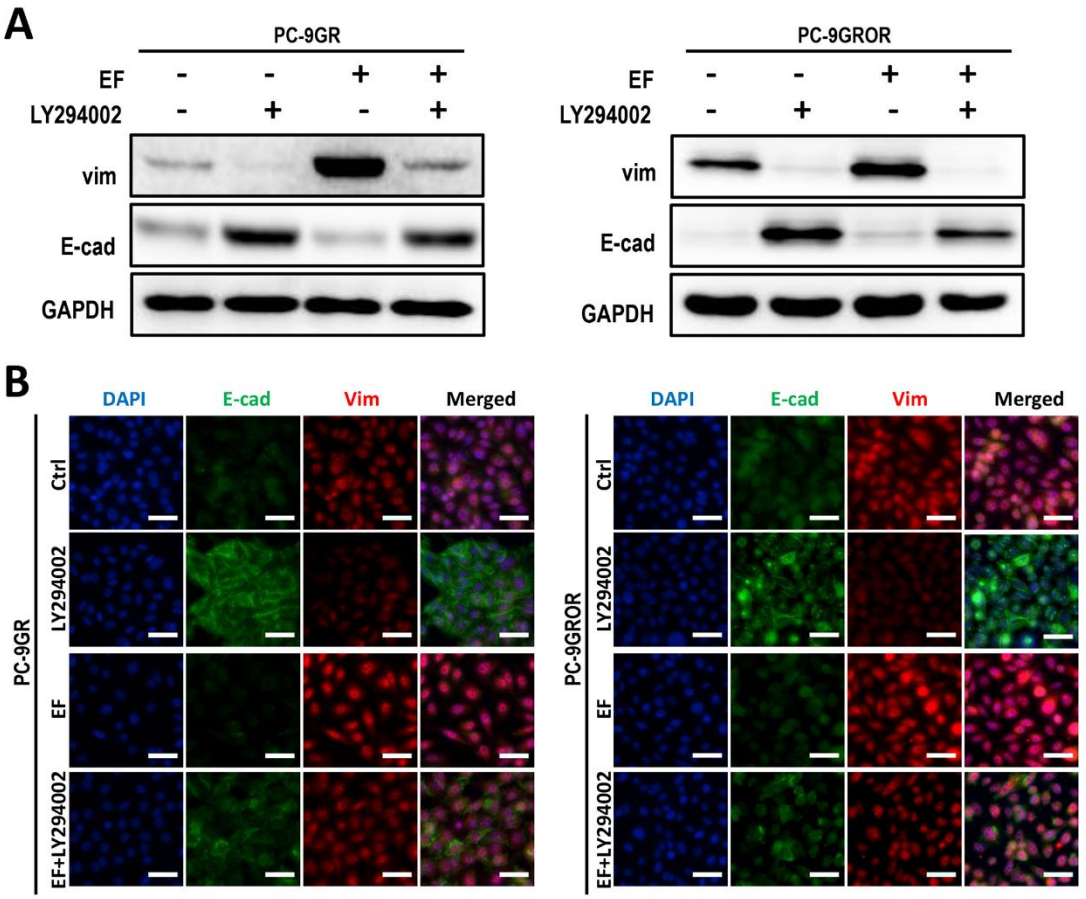

Figure 6. Working model of the current study. Endogenous EFs existed at the surface of EGFR-mutant lung tumor xenografts, and lung cancer cells showed electrotaxis. Furthermore, EFs induced EMT and AKT activation, and AKT activation was required for electrotaxis and EF-enhanced EMT of lung cancer

cells.